SSLP114 - semi-infinite plane Crack

Abstract

This test makes it possible to validate the computation of an asymptotic field by method XFEM. It is a question of checking if modelization XFEM represents the analytical solution accurately, of the fracture mechanics. This analytical field is the exact solution to the problem of opening in mode I of a plane crack.

The field is a square plate, cut until the medium by a horizontal crack. A loading is imposed on 4 edges to ensure rigorously an opening in mode I, in conformity with the analytical solution. One applies limiting conditions of standard “displacement” to not fissured edges, and of type “forces” on edge cut by crack.

To validate this approach, 3 modelizations are planned:

- Modelization a: one carries out a simple computation from linear elements (TRIA3) for a horizontal crack
- Modelization b: one C carries out a simple computation from quadratic elements (TRIA6) for a horizontal
- crack Modelization: one inclines crack to change the reference frame of the analytical formulas. To preserve the opening in mode I, one inclines the fields (forced and displacement) imposed on edges. On the one hand, one evaluates the incidence of the form of the field on the results, since in theory, the asymptotic equations do not depend on the geometry of the field in the reference frame of crack. In addition, one evaluates the robustness of computation with the degradation of conditioning.

One tests the stress intensity factors KI KII. For the mode I, one will have to find $KII=0$ and $KI\neq 0$, KI corresponding to the proportionality factor imposed on the fields solution (see paragraph [3]).

In the same way, one checks also the exactitude of the computation of the field of displacement calculated on the field, compared to the analytical solution.

1 Problem of reference

1.1 Geometry

Modelization a:
the structure 2D is a unit square plate ($LX=1$, $LY=1$), comprising a crack “leading” to a half-length [Figure 1.1-1]. The crack is right, horizontal and length $a=0,5$. One arbitrarily directs crack of flat rim towards the center.

The edges of the fields are noted in trigonometrical meaning:
- $LIG1$ indicate lower edge.
- $LIG2$ indicate flat rim.
- $LIG3$ indicate higher edge.
- $LIG4$ indicate left edge.

The 4 edges of the field are used to impose the limiting conditions. On edges not cut by crack ($LIG1$ $LIG2$, $LIG3$) one imposes limiting conditions of Dirichlet, using the analytical solution in displacement (see paragraph [3]).

Let us note that the flat rim ($LIG4$) cut by crack, generates a singularity at the intersection. One observes a jump of displacement corresponding to the opening of crack [Figure 2.3-1]. It is difficult to control this edge in displacement, since it is necessary analytically to clarify the jump condition on the upper lip and the lower lip of crack on the edge elements cut by crack. One circumvents this difficulty by imposing conditions of Neumann on this edge.

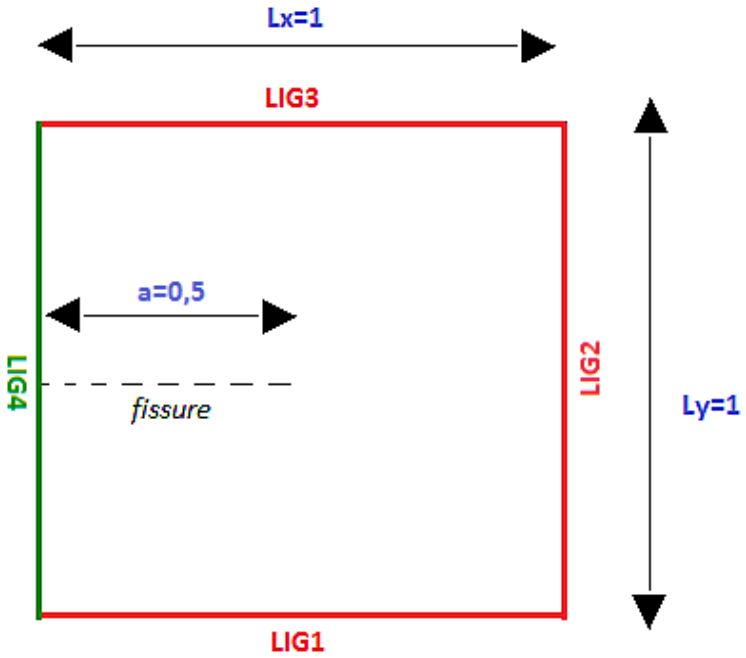

Figure 1.1-1: Geometry of the field

Modelization b:
Even geometry that modelization A.

Modélisation C:

One inclines crack of a variable angle such as $\alpha \epsilon \{0^\circ, 30^\circ, 60^\circ, 90^\circ, 120^\circ\}$ [Figure 1.1-2].

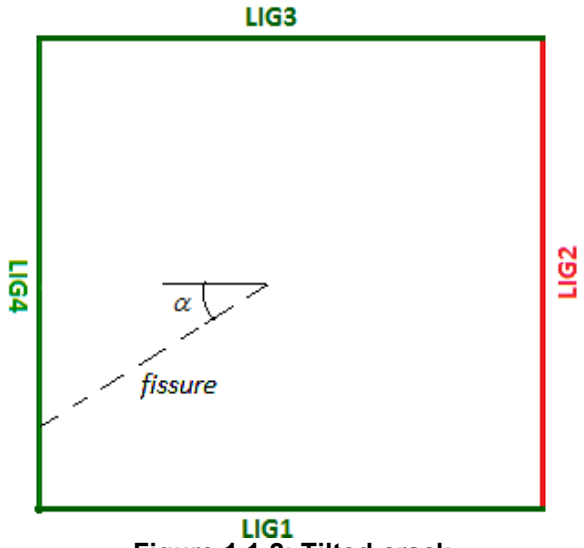

Figure 1.1-2: Tilted crack

Let us note that the crack lengthened. The new length is: $a = \frac{0,5}{max\left\{\left|\cos\left(\frac{\alpha \times \pi}{180}\right)\right|, \left|\sin\left(\frac{\alpha \times \pi}{180}\right)\right|\right\}}$.

1.2 Properties of the material

Modulus Young: $E = 10^5 Pa$
Poisson's ratio: $\nu = 0$

1.3 Boundary conditions and loadings

the loading is imposed thanks to mixed limiting conditions.

The not fissured edges are controlled in displacement, the fissured edge is controlled in force. In addition, the limiting conditions of Dirichlet (in displacement) fix structure and prevent the appearance of rigid modes.

In the modelizations A and B, the crack cuts only edge $LIG4$, One imposes a condition of Neumann on this edge and Dirichlet on 3 other edges (see [Figure 1.3-1]).

In the modelization C, one generalizes the preceding approach. For a slope higher than 45°, the crack cut either the lower edge ($LIG1$), or the higher edge ($LIG3$). To these two edges also one applies a condition of Neumann. One thus imposes a condition of Dirichlet on edge remaining ($LIG2$) to fix the rigid modes (see [Figure 1.3-2]). The limiting conditions being imposed symmetrically on horizontal crack ($\alpha = 0$), computations presented will be valid for $-135^\circ < \alpha < 135^\circ$

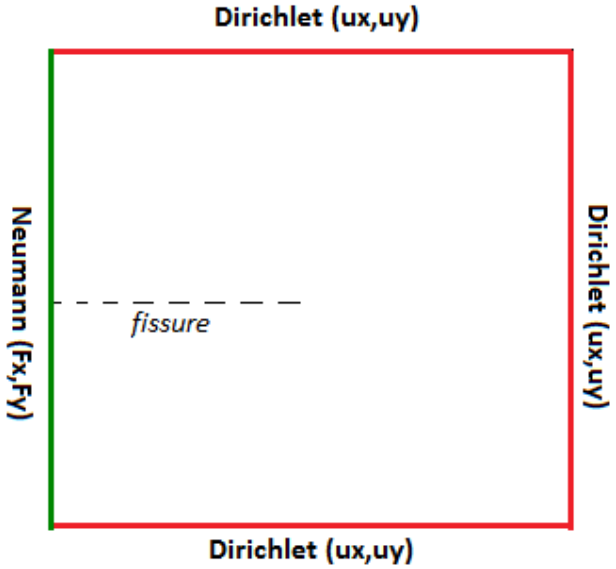

Figure 1.3-1: Mixed limiting conditions for the modelizations A and B

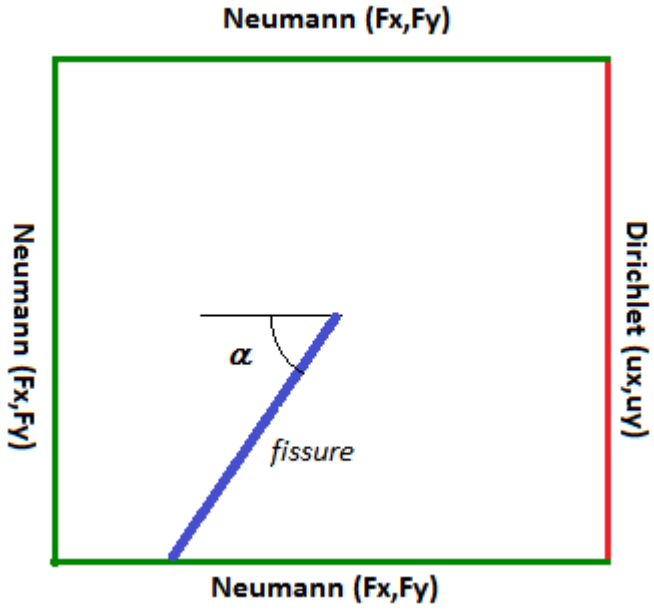

Figure 1.3-2: Mixed limiting conditions for the modelization C

imposed displacement corresponds to the exact analytical solution:

$$U_x=\frac{(1+\nu)}{E}\sqrt{\frac{r}{2\pi}}K_I\cos(\frac{\theta}{2})(3-4\nu-\cos\theta)$$

$$U_y=\frac{(1+\nu)}{E}\sqrt{\frac{r}{2\pi}}K_I\sin(\frac{\theta}{2})(3-4\nu-\cos\theta)$$

This solution depends on the polar coordinates related to the reference frame of crack [Figure 1.3-3]. In the literature ([9]), the direction of crack supports the axis $\vec{X}$. The axis $\vec{X}$ is directed bottom of crack towards outside. $\vec{Y}$ is orthogonal with $\vec{X}$, such as $(\vec{X},\vec{Y})$ forms a direct reference.

Consequently, it is necessary to carry out a basic change to adapt the valid analytical equations in the reference frame of crack, with a given reference. In particular, as the origin of the reference of the coordinates of meshes is selected with the left lower corner of the field, one relocates the polar coordinates:

θ is the polar angle: $\theta(x,y)=arctan2(y-0.5,x-0.5)$

r the radial distance: $r(x,y)=\sqrt{(x-0.5)^2+(y-0.5)^2}$

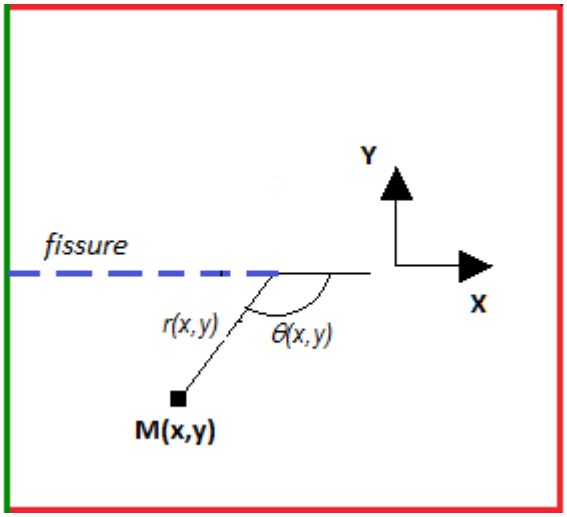

Figure 1.3-3: Local reference frame of the analytical formulas

Then, by the means of the tensor of the strains and the Hooke's law, one from of deduced the tensor from the stresses.

The computation tensor in the command file, follows the groundwork clarified below:

To compute: the tensor of the strains, one derives the functions $\phi_{i,k}(r,\theta)$:

$\phi_{1,k}(r,\theta)=\sqrt{r}\cos^k(\frac{\theta}{2})$ and $\phi_{2,k}(r,\theta)=\sqrt{r}\sin^k(\frac{\theta}{2})$

These functions form a base of the analytical solution, which is still written:

$$U_x=K_I\sum_{k\in\{1,3\}}a_{1,k}\phi_{1,k} \quad a_{1,1}=\frac{(1+\nu)}{E}\sqrt{\frac{r}{2\pi}}\times(4-4\nu) \quad a_{1,2}=0 \quad a_{1,3}=\frac{(1+\nu)}{E}\sqrt{\frac{r}{2\pi}}\times-2$$

$$U_y=K_I\sum_{k\in\{1,3\}}a_{2,k}\phi_{2,k} \quad a_{2,1}=\frac{(1+\nu)}{E}\sqrt{\frac{r}{2\pi}}\times(2-4\nu) \quad a_{2,2}=0 \quad a_{2,3}=\frac{(1+\nu)}{E}\sqrt{\frac{r}{2\pi}}\times 2$$

The derivatives partial of the functions $\phi_{i,k}(i\in\{1,2\})et(k\in\{1,3\})$ in the base $(\vec{X},\vec{Y})$ are written:

$$\frac{\partial \phi_{i,k}}{\partial x}=\frac{\partial \phi_{i,k}}{\partial r}\frac{\partial r}{\partial x}+\frac{\partial \phi_{i,k}}{\partial \theta}\frac{\partial \theta}{\partial x}=\frac{\partial \phi_{i,k}}{\partial r}\cos\theta-\frac{\partial \phi_{i,k}}{\partial \theta}\frac{\sin\theta}{r}$$

$$\frac{\partial \phi_{i,k}}{\partial y}=\frac{\partial \phi_{i,k}}{\partial r}\frac{\partial r}{\partial y}+\frac{\partial \phi_{i,k}}{\partial \theta}\frac{\partial \theta}{\partial y}=\frac{\partial \phi_{i,k}}{\partial r}\sin\theta+\frac{\partial \phi_{i,k}}{\partial \theta}\frac{\cos\theta}{r}$$

with,

$$\frac{\partial \phi_{1,k}}{\partial r}=\frac{1}{2\sqrt{r}}\cos^k\frac{\theta}{2}\quad \frac{\partial \phi_{1,k}}{\partial \theta}=-\frac{k}{2}\times\sqrt{r}\cos^{k-1}\frac{\theta}{2}\sin\frac{\theta}{2}$$

$$\frac{\partial \phi_{2,k}}{\partial r}=\frac{1}{2\sqrt{r}}\sin^k\frac{\theta}{2}\quad \frac{\partial \phi_{2,k}}{\partial \theta}=\frac{k}{2}\times\sqrt{r}\sin^{k-1}\frac{\theta}{2}\cos\frac{\theta}{2}$$

By summation, one deduces: $\frac{\partial U_i}{\partial x_j}=K_I\sum_{k\in\{1,3\}}a_{i,k}\frac{\partial \phi_{i,k}}{\partial x_j}$

with the strain tensor, $\epsilon_{ij}=\frac{1}{2}(\frac{\partial U_i}{\partial x_j}+\frac{\partial U_j}{\partial x_i})$

Lastly, the Hooke's law, $\sigma_{ij}=\frac{E}{(1+\nu)}(\epsilon_{ij}+\frac{\nu}{(1-2\nu)}(\epsilon_{11}+\epsilon_{22})\delta_{ij})$

Then, one projects the tensor of the stresses to deduct the density of force from it to be applied to flat rim ($LIG4$), of “outgoing” norm $-\vec{X}$.

The force to be applied is: $\vec{F}=\underline{\underline{\sigma}}.-\vec{X}$

It comes: $F_x=-\sigma_{xx}=-\sigma_{11}$ and $F_y=-\sigma_{xy}=-\sigma_{12}$

Modelization a:
Compared to the reference frame of crack, the axes “aster” are directed in the same meaning. The fields of displacement Ux and Uy reference are applied to edges LIG1, LIG2, LIG3:

$$U_x=\frac{E}{2(1+\nu)}\sqrt{\frac{r}{2\pi}}K_I\cos(\frac{\theta}{2})(3-4\nu-\cos\theta)$$

$$U_y=\frac{E}{2(1+\nu)}\sqrt{\frac{r}{2\pi}}K_I\sin(\frac{\theta}{2})(3-4\nu-\cos\theta)$$

In the same way the strain tensor reference is preserved. One thus applies the same density of force clarified above to edge $LIG4$.

$$F_x=-\sigma_{xx}\quad F_y=-\sigma_{xy}$$

Modelization b:
Same equations as modelization A.

Modélisation C:

One inclines crack of an angle of $\alpha \epsilon \{0^{\circ},30^{\circ},60^{\circ},90^{\circ},120^{\circ}\}$.

This rotation impacts **the polar angle**, **the field of displacement** and **the tensor of the stresses**. These quantities carry out a rotation of an angle α, compared to the fixed reference of the code aster.

$\theta \rightarrow \theta - \alpha$

However this transformation of the polar angle is not valid for all the angles, because the definition of the polar angle is not continuous. In the local reference frame, on both sides of crack one observes an angular jump of 2π : lower lip with the upper lip one passes from $-\pi$ to π.

Consequently, the rotation of crack must also propagate this angular discontinuity. All the angles swept by the crack (grayed zone cf [Figure 1.3-4] and [Figure 1.3-5]) during rotation, undergo an angular jump of -2π or 2π,

If $\alpha > 0$ (the rotation of crack is carried out downwards)
- In the zone $-\pi < \theta < -\pi + \alpha$ one a: $\theta \rightarrow \theta - \alpha + 2\pi$
- In the zone $\pi > \theta > -\pi + \alpha$ one a: $\theta \rightarrow \theta - \alpha$

If $\alpha < 0$ (the rotation of crack is carried out upwards)
- In the zone $\pi > \theta > \pi + \alpha$ one a: $\theta \rightarrow \theta - \alpha - 2\pi$
- In the zone $-\pi < \theta < \pi + \alpha$ one a: $\theta \rightarrow \theta - \alpha$

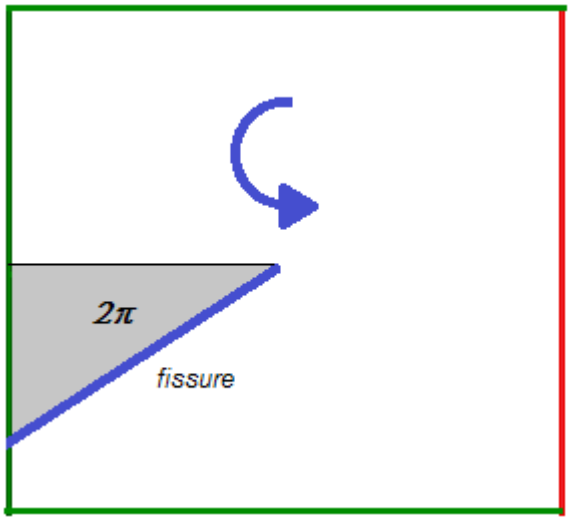

Figure 1.3-4: Angular field of jump (positive)

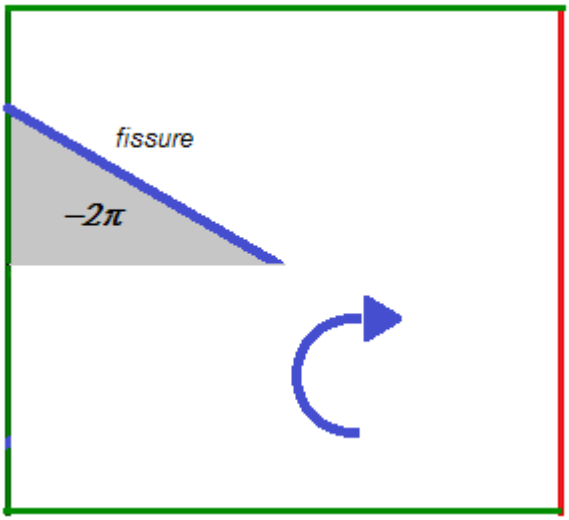

Figure 1.3-5: Angular field of jump (negative)

$\vec{U} \to R_\alpha \vec{U}$ where R_α is the matrix of rotation of angle α with $R_\alpha = \begin{bmatrix} \cos(\alpha) & -\sin(\alpha) \\ \sin(\alpha) & \cos(\alpha) \end{bmatrix}$

Consequently,

$$\vec{U} \to \begin{bmatrix} \cos(\alpha) U_x - \sin(\alpha) U_y \\ \sin(\alpha) U_x + \cos(\alpha) U_y \end{bmatrix}$$

the tensor of the strains is also impacted by rotation:

$$\underline{\underline{\sigma}} \to R_\alpha \underline{\underline{\sigma}} R_{-\alpha}$$

$$\underline{\underline{\sigma}} \to \begin{bmatrix} \cos(\alpha) & -\sin(\alpha) \\ \sin(\alpha) & \cos(\alpha) \end{bmatrix} \begin{bmatrix} \sigma_{xx} & \sigma_{xy} \\ \sigma_{xy} & \sigma_{yy} \end{bmatrix} \begin{bmatrix} \cos(\alpha) & \sin(\alpha) \\ -\sin(\alpha) & \cos(\alpha) \end{bmatrix}$$

$$\underline{\underline{\sigma}} \to \begin{bmatrix} \cos(\alpha) & -\sin(\alpha) \\ \sin(\alpha) & \cos(\alpha) \end{bmatrix} \begin{bmatrix} \cos(\alpha)\sigma_{xx} - \sin(\alpha)\sigma_{xy} & \sin(\alpha)\sigma_{xx} + \cos(\alpha)\sigma_{xy} \\ \cos(\alpha)\sigma_{xy} - \sin(\alpha)\sigma_{yy} & \sin(\alpha)\sigma_{xy} + \cos(\alpha)\sigma_{yy} \end{bmatrix}$$

From where the final writing of the stress tensor:

$$\underline{\underline{\sigma}} \to \begin{bmatrix} \cos(\alpha)^2\sigma_{xx} - \sin(2\alpha)\sigma_{xy} + \sin(\alpha)^2\sigma_{yy} & -\frac{1}{2}\sin(2\alpha)(-\sigma_{xx} + \sigma_{yy}) + \cos(2\alpha)\sigma_{xy} \\ -\frac{1}{2}\sin(2\alpha)(-\sigma_{xx} + \sigma_{yy}) + \cos(2\alpha)\sigma_{xy} & \sin(\alpha)^2\sigma_{xx} + \sin(2\alpha)\sigma_{xy} + \cos(\alpha)^2\sigma_{yy} \end{bmatrix}$$

It is checked that rotation preserves the symmetry of the tensor and the trace, $tr(\underline{\underline{\sigma}}) = \sigma_{xx} + \sigma_{yy}$

In the programming of the command file, the horizontal crack is a typical case of tilted crack: all the equations depend on an unspecified α slope. To find the modelization A and B, it is enough to make $\alpha = 0°$.

1.4 Reference solution

One imposes $K_I = 1$.

In the reference frame related to crack, the analytical equations become:

$$U_x = \frac{E}{2(1+\nu)}\sqrt{\frac{r}{2\pi}}\cos(\frac{\theta}{2})(3 - 4\nu - \cos\theta)$$

$$U_y = \frac{E}{2(1+\nu)}\sqrt{\frac{r}{2\pi}}\sin(\frac{\theta}{2})(3 - 4\nu - \cos\theta)$$

By linearity of the equations, the tensor of the strains is affected by the same proportionality factor.

By construction, it does not exist of mode II. In other words, one tests $K_{II} = 0$.

1.5 Bibliographical references

[1] GENIAUT S., MASSIN P.: eXtended Finite Method Element, Handbook of reference of *Code_Aster*, [R7.02.12]

[2] Rice, J.R. (1968), “A path independent integral and the approximate analysis of strain concentration by notches and aces”, *Newspaper of Applied Mechanics* **35**: 379-386

[3] Satzi, Belytschko: Year extended Finite Element Method with Higher-Order Elements for Curved Aces

[4] LABORDE P., APPLE TREE J., FOX Y., SALAUN Mr., “High-order extended finite element method for cracked domains”, International Newspaper for Numerical Methods in Engineering, vl.
64, pp. 354-381, 2005

2 Modelization A

In this modelization D_PLAN, the plate is fissured on a half-length. The crack is described by method XFEM. The crack is enriched geometrically, on a radius $R_{ENRI}=0,1$.

The elements are linear of type TRIA3.

2.1 Characteristics of the mesh

the unit square is with a grid regularly [Figure 2.1-1]. To build the mesh, one leans on a regular squaring 100×100 .

NUMBER OF NODES: 10201

NUMBER OF MESHES: 20400
TRIA3: 20000

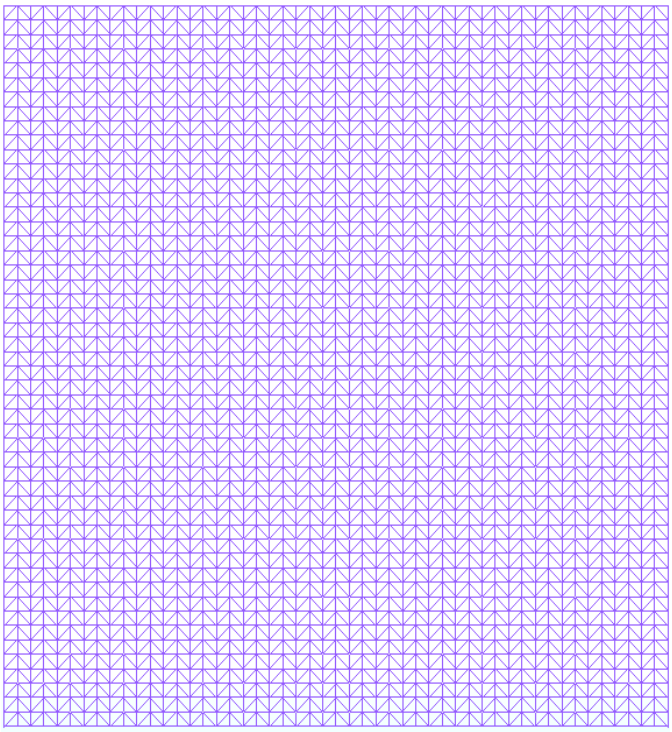

Figure 2.1-1: Mesh with element-triangles

2.2 Quantities tested and Quantities

2.2.1 results tested:

For this horizontal crack, one tests the value of the stress intensity factors K_I and K_{II} data by CALC_G.

For the method $G-thêta$ (command CALC_G), one selected the following contour of field theta:

$R_{inf}=0,1\,a$ and $R_{\sup}=0,3\,a$ where a is the length of crack.

In addition, one tests the field of displacement calculated by Code_Aster. Instead of carrying out a local test on some meshes by TEST_RESU, one tests the field of displacement on a large number of meshes. An arbitrary zone of test was delimited in the field [Figure 2.2.1-1].

In practice, one compares: $\left\| U^{calc} - U^{ana} \right\|_{L_2} < tolerance \times \left\| U^{ana} \right\|_{L_2}$.

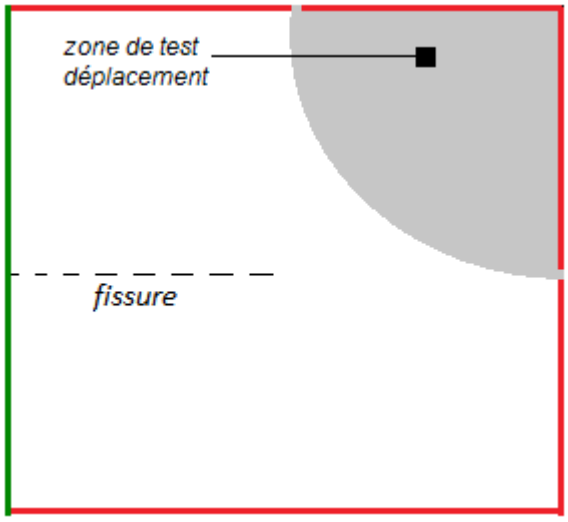

Figure 2.2.1-1: definition of the GROUP_MA of test

2.2.2 Results:

Test of the stress intensity factors:

Identification	Reference	Tolerance
CALC_G		
K1	1.00	1.0%
K2	0.00	1.0%
G	1,0 10-5	1.0%

Test of the norme_L2 of the error on the field of displacement: $\left\| U^{calc} - U^{ana} \right\|_{L_2} < tolerance \times \left\| U^{ana} \right\|_{L_2}$

Identification	Reference	Tolerance
POST_ELEM		
NORMALIZES	0.00	0.1%

2.3 complementary Results:

On [Figure 2.3-1], the field of displacement is represented with amplification of the jump of displacement to the interface. It is noted that the crack opens rigorously in $mode\ I$, as expected.

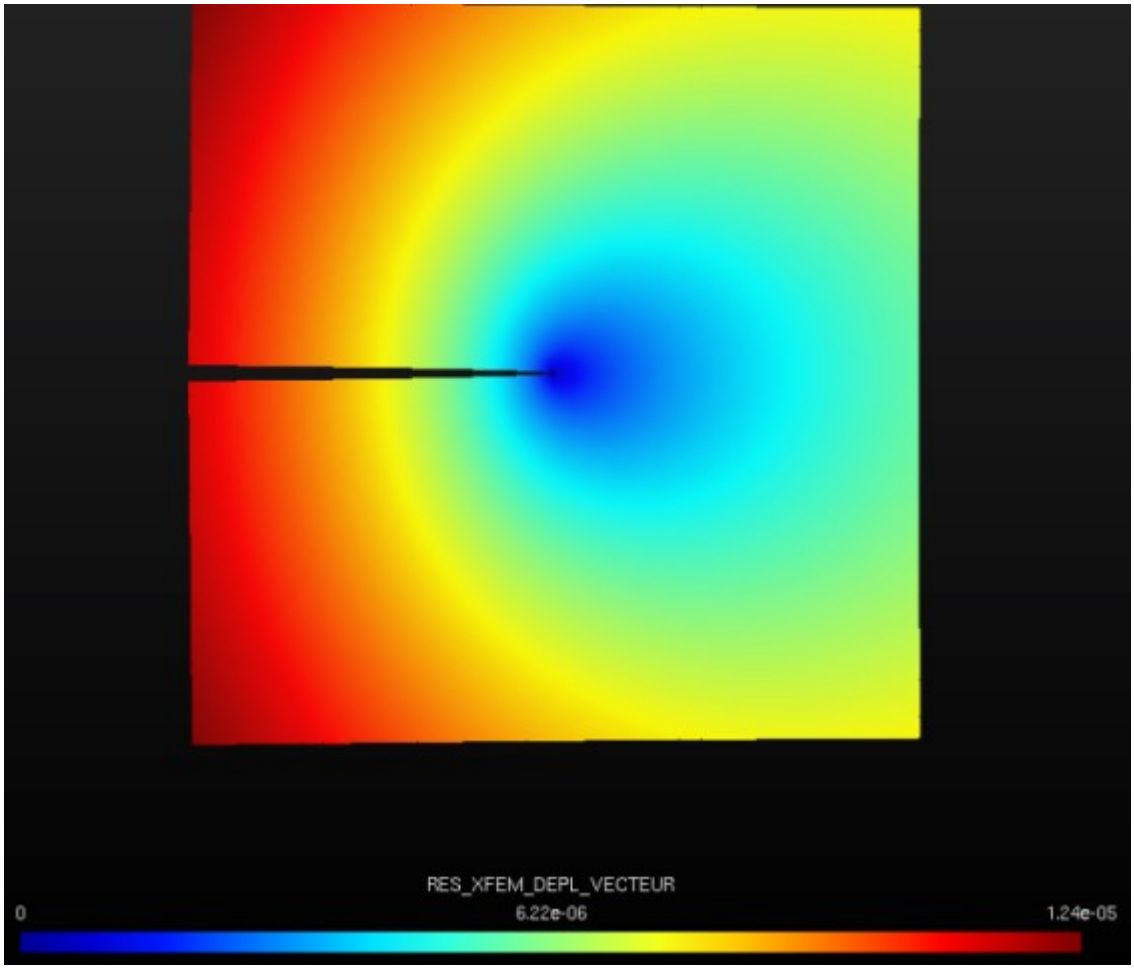

Figure 2.3-1: Field of displacement (with offset)

3 Modelization B

Modelization D_PLAN, with method XFEM to represent crack. Quadratic elements TRIA6.

3.1 Characteristics of the mesh

the unit square is with a grid regularly [Figure 2.1-1]. One preserves the refinement of the preceding modelization.

NUMBER OF NODES: 40401

NUMBER OF MESHES: 20400
TRIA6: 20000

3.2 Quantities tested and results

One tests the same quantities as in modelization A.

Test of the stress intensity factors:

Identification	Reference	Tolerance
CALC_G		
K1	1.00	1.0%
K2	0.00	1.0%
G	1,0 10-5	1.0%

Test of the norm $L2$ of the error on the field of displacement:

Identification	Reference	Tolerance
POST_ELEM		
NORMALIZES	0.00	0.1%

4 Modelization C

Modelization D_PLAN, with method XFEM to represent crack. Quadratic elements TRIA3.

4.1 Characteristics of the mesh

the unit square is with a grid regularly [Figure 2.1-1]. One preserves the refinement of the preceding modelizations.

NUMBER OF NODES: 10201

NUMBER OF MESHES: 20400
TRIA3: 20000

4.2 Quantities tested and results

the same quantities are tested that in modelization A. One checks the stress intensity factors and the field of displacement on part of the field compared to the analytical values.

that for the definition of the zone of test, for a variable slope, one generalizes the approach of modelization A. According to the slope of crack, one tests the corner of the field opposed to crack (see [Figure 4.2-1] and [Figure 4.2-2]).

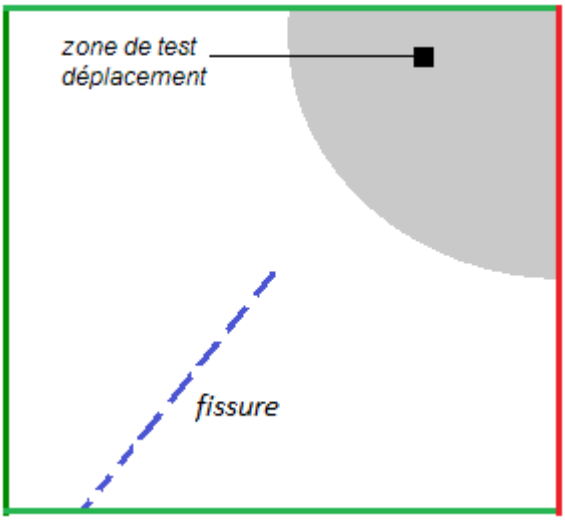

Figure 4.2-1: Definition of the GROUP_MA of let us testNotons

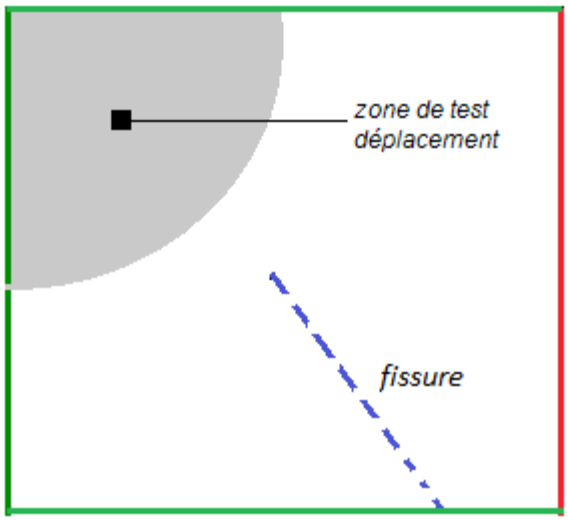

Figure 4.2-2: Definition of the GROUP_MA of test

Test of the stress intensity factors:

Identification	Reference	Tolerance
CALC_G		
K1	1.00	1.0%
K2	0.00	1.0%
G	1,0 10-5	1.0%

Test of the norm $L2$ of the error on the field of displacement:

Identification	Reference	Tolerance
POST_ELEM		
NORMALIZES	0.00	1.0%

4.3 complementary Results:

Ci below, one represents the field of displacement (with offset) for a variable slope of crack.

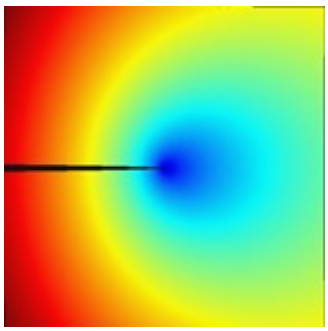
alpha=0°

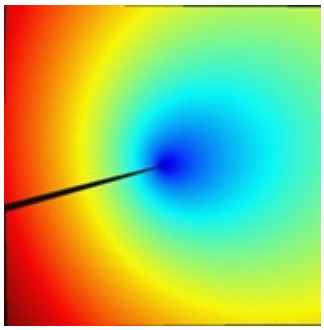
alpha=15°

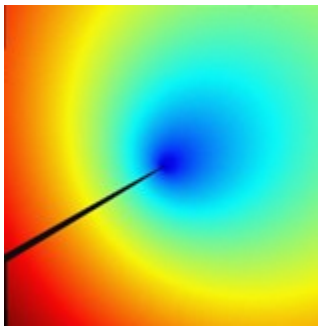
alpha=30°

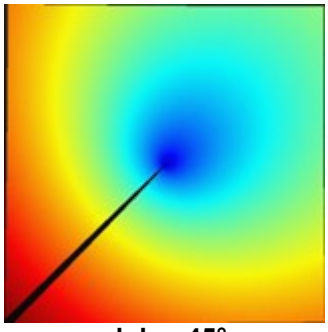
alpha=45°

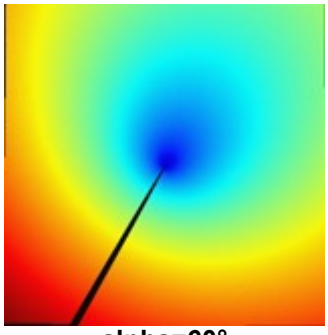
alpha=60°

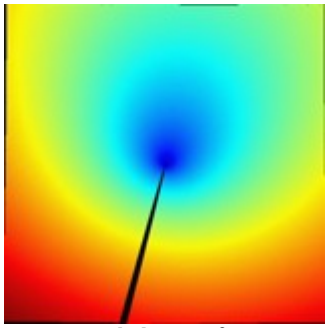
alpha=75°

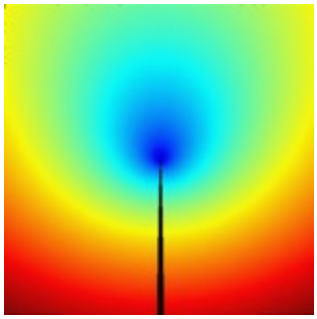
alpha=90°

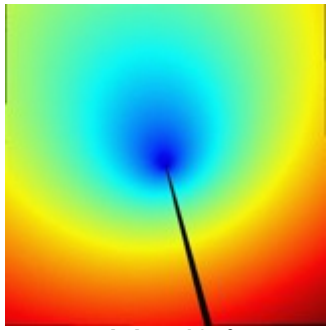
alpha=105°

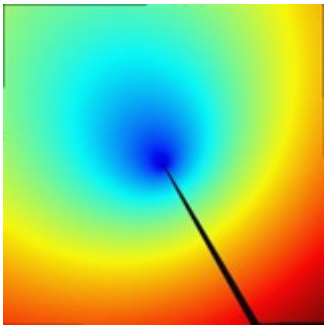
alpha=120°

5 Summaries of the results

the modelizations A, B and C show that method XFEM makes it possible to find the asymptotic field of the theory for a crack opening in mode I. It is noted that the field of displacement is accurately represented since, in particular, one finds the analytical values of the stress intensity factors.

In the paragraph [15], one restored the evolution of the field of displacements according to the angle of inclination, on a great angular beach. One shows thus that the field calculated displacement remains invariant in the local reference frame related to crack: the asymptotic field "follows" the motion of crack, in accordance with the theory. Consequently, the geometry of the field in the reference frame of crack, the regularity and the "directionnality" of the mesh, do not affect the accuracy of computations of the benchmark, with linear elements.

Moreover, one does not note the appearance of a zone of transition between the conditions from limits from Dirichlet and Neumann. For example in the modelization C, the test on the norm $L2$ of the error in displacement, is carried out on the corner undergoing at the same time a loading of Neumann and a condition of
Dirichlet. The displacement calculated by Aster "sticks" to the analytical solution. Would it as have to be made sure as the same applies to stress field? Developments in the code_Aster should set up a computation of the norm in energy to confirm these observations.

However, there exist 2 limitations with the validation presented above:

- On the one hand, the slope "ad infinitum" of crack is not possible in our model. In the modelization C, the angle of inclination is understood enters $-135°$ and $135°$ because of the limiting condition of Dirichlet on one of edges of the field. Being given the symmetry of the problem, to continue this study on the rest of the trigonometrical circle does not appear relevant.
- In addition, the modelization B watch which a validation is possible with quadratic elements. However, one indicates a significant degradation of conditioning.